

Resonant transport in coupled quantum wells: A probe for scattering mechanisms

Y. Berk

School of Physics and Astronomy, Raymond and Beverly Sackler Faculty of Exact Sciences, Tel Aviv University, Tel Aviv 69978, Israel

A. Kamenev

Department of Condensed Matter, The Weizmann Institute of Science, Rehovot 76100, Israel

A. Palevski

School of Physics and Astronomy, Raymond and Beverly Sackler Faculty of Exact Sciences, Tel Aviv University, Tel Aviv 69978, Israel

L. N. Pfeiffer and K. W. West

AT&T Bell Laboratories, Murray Hill, New Jersey 07974

(Received 21 July 1994)

We present a microscopic theory and experimental results concerning resistance resonance in two tunneling coupled quantum wells with different mobilities. The shape of the resonance appears to be sensitive to the small angle scattering rate on remote impurities and to the electron-electron scattering rate. This allows the extraction of scattering parameters directly from the transport measurements. The negative resonance in a Hall coefficient is predicted and observed.

The resistance resonance (RR) in two coupled quantum wells (QW) with different mobilities was recently suggested and discovered experimentally.¹ The basic physical idea of this phenomenon is the following. One studies the *in-plane* resistance of two tunneling coupled QW's as a function of a relative position of their quantized energy levels. Each current lead is contacted to both QW's. The energy levels are shifted by applying the voltage to the capacitively coupled gate (see device diagram on the inset to Fig. 1). If the energy levels are far from each other, the tunneling is suppressed and the resulting resistance is given by, $R_{\text{off}} \sim (\tau_1^{\text{tr}} + \tau_2^{\text{tr}})^{-1}$ (two resistors connected in parallel), where τ_i^{tr} are the transport mean free times in the corresponding wells. The situation, however, is remarkably different once the system is brought into the resonance (energy levels coincide). In this case, the wave functions form symmetric and antisymmetric subbands, split by a tunneling gap. As any electron is completely delocalized between two wells, the scattering rate in each of these subbands is $(\tau^{\text{tr}})^{-1} = (2\tau_1^{\text{tr}})^{-1} + (2\tau_2^{\text{tr}})^{-1}$. The resulting resistance is given by $R_{\text{res}} \sim (2\tau^{\text{tr}})^{-1}$. If the transport scattering rates of two QW's are different, the resistance as a function of the gate voltage exhibits the resonance, whose relative amplitude is

$$(R_{\text{res}} - R_{\text{off}})/R_{\text{off}} = (\tau_1^{\text{tr}} - \tau_2^{\text{tr}})^2 / 4\tau_1^{\text{tr}}\tau_2^{\text{tr}} \equiv A. \quad (1)$$

This effect was indeed observed and reported in a number of publications.¹⁻³ In this paper, we present a microscopic model of the RR, which includes elastic scattering on a long-range remote impurity potential. We also report the experimental measurements of the RR shape and its temperature dependence, and we analyze them within the presented theoretical model. In addition, we have calculated and measured the Hall coefficient in coupled QW's. We show that at the resonant conditions the Hall coefficient exhibits a local minimum, which may be well

understood on a basis of a classical two-band model.

The main messages which follow from the present investigation are the following: (i) at low temperature, the width of the RR is determined by a small angle scattering time on remote impurities, providing an independent way of measuring the small angle scattering time in a pure transport experiment; (ii) the temperature dependence of the RR indicates that a shape of the resonance is sensitive to the electron-electron interactions, allowing determination of the electron-electron scattering rate; (iii) the resonance in a Hall coefficient is predicted and demonstrated experimentally.

We first present a theoretical model of a transport in two coupled QW's. In a basis of local states of each QW, the Hamiltonian of the system may be written in the following matrix form: $H = \hat{a}_{\mathbf{k}}^\dagger \hat{H}_{\mathbf{k},\mathbf{p}} \hat{a}_{\mathbf{p}}$, where

$$\hat{H}_{\mathbf{k},\mathbf{p}} = \delta_{\mathbf{k}\mathbf{p}} \begin{pmatrix} \epsilon_1 + (\mathbf{p} - e\mathbf{A})^2 / (2m^*) & \Delta/2 \\ \Delta^*/2 & \epsilon_2 + (\mathbf{p} - e\mathbf{A})^2 / (2m^*) \end{pmatrix} + \begin{pmatrix} U_1(\mathbf{p} - \mathbf{k}) & 0 \\ 0 & U_2(\mathbf{p} - \mathbf{k}) \end{pmatrix}, \quad (2)$$

and \mathbf{k}, \mathbf{p} are two-dimensional (2D) momentum of the electrons. In the last equation $\epsilon_i(V_G)$ are bare quantized levels of corresponding wells, which are functions of a gate voltage, V_G . The tunneling coupling (gap), Δ , is assumed to be in-plane momentum conserved and energy independent. A vector potential of the external field (electric and magnetic) is denoted by $\mathbf{A} = \mathbf{A}(\mathbf{r}, t)$. Finally, $U_i(\mathbf{p} - \mathbf{k})$ represents the elastic disorder in each layer. We shall assume that impurity potentials in different wells are uncorrelated. Inside each QW an impurity potential has a finite correlation length and may be characterized by the two parameters: the single particle (or small angle) scattering time and the two particle (or transport) scattering time (hereafter we employ the energy units for various scattering rates, $\hbar = 1$)

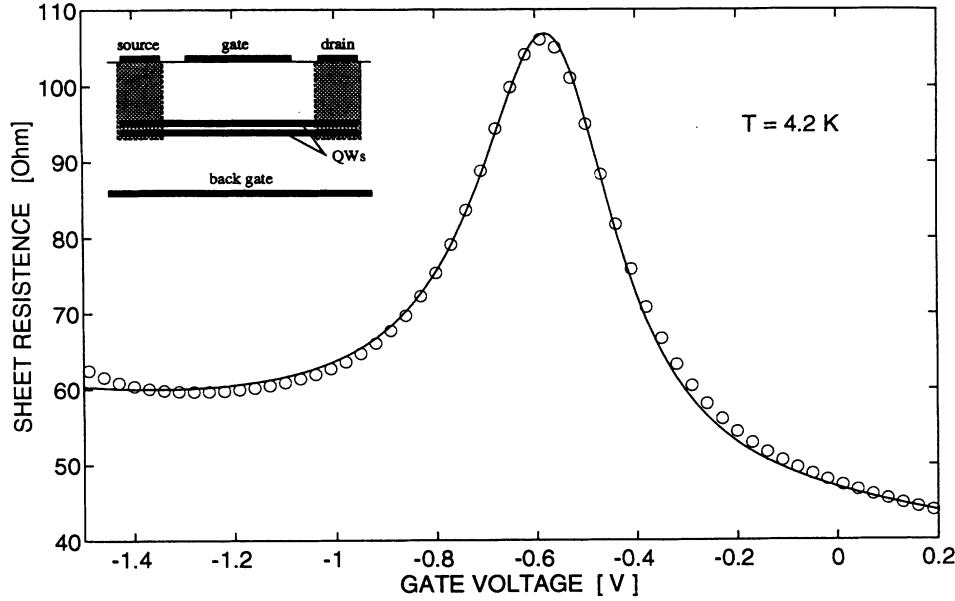


FIG. 1. Resistance resonance (RR) curves: circles—experimental data, solid line—theoretical calculation. The inset—schematic diagram of the device.

$$\frac{1}{\tau_i} \propto \int |U_i(\mathbf{p})|^2 d\Omega; \quad \frac{1}{\tau_i^{\text{tr}}} \propto \int |U_i(\mathbf{p})|^2 (1 - \cos \theta) d\Omega, \quad (3)$$

where the integrations are carried out over the Fermi circles.

Now the model is specified completely and we apply it first to the calculation of a linear conductance. Using the Kubo formula, one has

$$\sigma = \int d\epsilon \frac{f(\epsilon) - f(\epsilon + \omega)}{2\pi S \omega} \text{Tr} \langle \hat{I}_{\mathbf{p}} \hat{G}_{\mathbf{p},\mathbf{k}}^+(\epsilon + \omega) \hat{I}_{\mathbf{k}} \hat{G}_{\mathbf{k},\mathbf{p}}^-(\epsilon) \rangle, \quad (4)$$

where Tr stays for both matrix and momentum indexes; S is an area of the structure. A current operator, $\hat{I}_{\mathbf{p}}$, is $e\mathbf{p}/m$ times a unit matrix (if all contacts are attached to the both wells). Retarded and advanced Green functions of a system are defined as

$$\hat{G}_{\mathbf{p},\mathbf{k}}^{\pm}(\epsilon) = \langle \mathbf{p} | (\epsilon - H \pm i\eta)^{-1} | \mathbf{k} \rangle. \quad (5)$$

Constructing the perturbation expansion over the impurity potential [the second term in Eq. (2)], and solving the Dyson equation for an average Green function, one obtains to the leading order in $(\epsilon_F \tau_i)^{-1}$,⁴

$$\langle \hat{G}_{\mathbf{p},\mathbf{k}}^{\pm}(\epsilon) \rangle = \delta_{\mathbf{k}\mathbf{p}} \begin{pmatrix} \epsilon - \epsilon_1 - \epsilon_{\mathbf{p}} \pm i/2\tau_1 & \Delta/2 \\ \Delta^*/2 & \epsilon - \epsilon_2 - \epsilon_{\mathbf{p}} \pm i/2\tau_2 \end{pmatrix}^{-1}.$$

Note that a tunneling coupling is taken into account in a nonperturbative fashion, hence the final results should not be restricted by lowest orders in Δ . The conductivity, according to Eq. (4) is given by a diagram Fig. 2(a), where the shaded triangle represents the renormalized current vertex. To evaluate the latter one should solve the matrix integral equation schematically depicted on Fig. 2(c).⁴ The calculation gives the following result for the zero-frequency resistance ($R = \sigma^{-1}$)

$$R = \frac{R_1 R_2}{R_1 + R_2} \left[1 + A \frac{|\Delta|^2 \tau^{\text{tr}} \tau^{-1}}{(\epsilon_1 - \epsilon_2)^2 + |\Delta|^2 \tau^{\text{tr}} \tau^{-1} + \tau^{-2}} \right]; \quad (6)$$

$$1/\tau = (1/2\tau_1) + (1/2\tau_2); \quad 1/\tau^{\text{tr}} = (1/2\tau_1^{\text{tr}}) + (1/2\tau_2^{\text{tr}}),$$

where $R_i = (e^2 \hbar n_i \tau_i^{\text{tr}} / m)^{-1}$ are resistances of each well and the asymmetry coefficient, A , is defined by Eq. (1). The result, Eq. (6), is valid if all relevant energies are much less than the Fermi energy, ϵ_F ; this implies that the concentrations of carriers in two QW's are close to each other, $|n_1 - n_2| \ll n_i$. For relatively clean case, $|\Delta|^2 \gg (\tau \tau^{\text{tr}})^{-1}$, Eq. (6) confirms our qualitative conclusions, drawn in the beginning. In the dirty case (the opposite limit), the height of the resonance is suppressed. Note, that the width of the resonance depends on the small angle scattering time, τ , although the resistances of each well are fully determined by the transport times, τ_i^{tr} . The physical nature of this fact is the following. Any elastic scattering process (e.g., the small angle scattering) leads to a mixing between the states of symmetric and antisymmetric subbands (according to classification in clean wells). Not too far from the exact resonance (say

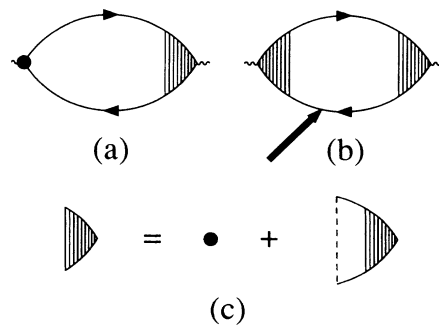


FIG. 2. Diagrams for a conductivity (a) and a Hall coefficient (b), current vertex renormalization due to a small angle scattering (c). Full circle—bare current vertex; dashed line—impurity scattering.

$\epsilon_1 - \epsilon_2 \approx \Delta$) the wave functions of clean wells would be practically localized in one of the wells (e.g., “symmetric” in the upper one and “antisymmetric” in the lower one). In this case, they are sensitive only to scatterers in the corresponding well and the resonance is destroyed. The mixing due to small angle scattering changes the situation, making the exact eigenfunction of the dirty wells delocalized. As a result, the resonance appears to be broader than in the case without small angle scattering. Unlike the width of the resonance, its relative amplitude is mostly determined by the transport quantities [at least for $|\Delta|^2 \gg (\tau\tau^{\text{tr}})^{-1}$] and is not sensitive to the single particle scattering rate.

The Hall coefficient is given by the two diagrams, one of which is depicted in a Fig. 2(b).^{5,6} We present here only the result for the short range impurity potential ($\tau_i = \tau_i^{\text{tr}}$)

$$R_H = \frac{R_{H,2}R_1^2 + R_{H,1}R_2^2}{(R_1 + R_2)^2} \left[1 - A \frac{2\tau_1\tau_2}{\tau_1^2 + \tau_2^2} |\Delta|^2 \right. \\ \left. \times \frac{(\epsilon_1 - \epsilon_2)^2 + |\Delta|^2 + 3\tau^{-2}}{[(\epsilon_1 - \epsilon_2)^2 + |\Delta|^2 + \tau^{-2}]^2} \right], \quad (7)$$

where $R_{H,i} = (n_i e)^{-1}$ is a Hall coefficient of each QW. We shall discuss the physics of the last expression later, when presenting the experimental results.

The double QW structure was grown on N^+ GaAs substrate by molecular-beam epitaxy and consisted of two GaAs wells 139 Å width separated by a 40 Å $\text{Al}_{0.3}\text{Ga}_{0.7}\text{As}$ barrier. The electrons were provided by remote δ -doped donor layers set back by 250 Å and 450 Å spacer layers from the top and the bottom well correspondingly. In order to obtain the difference in the mobilities, an enhanced amount of impurities was introduced at the upper edge of the top well (Si, 10^{10} cm^{-2}). The schematic cross-section of the device may be found in Ref. 1. Measurements were done on 10 μm wide and 200- μm -long channels with Au/Ge/Ni Ohmic contacts. Top and bottom gates were patterned using the standard photolithography fabrication method. The top Schottky gate covered 150 μm of the channel (see inset to Fig. 1). The data were taken using a lock-in four terminal techniques at $f = 11 \text{ Hz}$. The voltage probes connected to the gated segment of the channel were separated by 100 μm .

The application of the upper gate voltage allows us to sweep the potential profile of the QW's through the resonant configuration. The variation of the resistance vs upper gate voltage is plotted in Fig. 1 (circles). The data were obtained at the $T = 4.2 \text{ K}$ for the bottom gate voltage $V_{\text{GB}} = 0.5 \text{ V}$. The resistance resonance is clearly observed at $V_G \approx -0.6 \text{ V}$. In order to compare the experimental data with the theoretical formula, Eq. (6), one has to establish the correspondence between the gate voltages and the energy levels, ϵ_i . The latter was found, using the known density of states and dc capacitances between the QW's and corresponding gate electrodes. The experimental values of these capacitances were established using the Hall measurements in the regime of the complete depletion of the top QW, and are given by $C_1 = 4.53 \times 10^{-8} \text{ F cm}^{-2}$ for the upper

gate and $C_2 = 1.79 \times 10^{-8} \text{ F cm}^{-2}$ for the bottom gate, which are extremely close to the theoretical estimates. The complementary measurements of the resistance and Hall coefficient far from the resonance allow us to determine the following parameters of our structure (as grown, i.e., $V_G = V_{\text{GB}} = 0$ and $T = 4.2 \text{ K}$): $\mu_1 = 47\,000 \text{ cm}^2/\text{V sec}$,⁷ $\mu_2 = 390\,000 \text{ cm}^2/\text{V sec}$, $n_1 = 4.7 \times 10^{11} \text{ cm}^{-2}$, $n_2 = 2.5 \times 10^{11} \text{ cm}^{-2}$. The values of these parameters for each gate voltage were found independently and used for the fits. The quantum mechanical calculation of the tunneling gap results in $\Delta = 0.55 \text{ meV}$; a very similar value for an identical structure was found experimentally.⁸ The only parameter, which was not determined by independent measurement is the small angle scattering rate, τ^{-1} . The best fit (solid line in Fig. 1) was achieved for $\tau^{-1} = 1.3 \text{ meV}$. This value implies the ratio between transport and small angle scattering times to be equal to 4.7, which is in a good agreement with the measurements, using Shubnikov–de Haas oscillations on a 2D gas with approximately the same mobility.⁹ To our knowledge, this is the first time when the small angle scattering rate was determined in a pure (zero magnetic field) transport experiment.

The same fitting procedure was applied to a set of the resistance resonance data within the temperature range 4.2 – 60 K, see Fig. 3. Among the independently measured parameters, only the mobility of a clean QW, μ_2 , exhibits pronounced temperature dependence, which is consistent with previously reported experimental data.¹⁰ The temperature dependence of the fitting parameter, $\tau^{-1}(T)$, is plotted by circles in an inset to Fig. 3. At low temperature it may be well approximated by the following relation (the solid line in the inset):

$$\tau^{-1}(T) = \tau^{-1}(0) + 3.0 (k_B T)^2 / \epsilon_F, \quad (8)$$

where $\epsilon_F = 10.9 \text{ meV}$ is the Fermi energy and $\tau^{-1}(0) = 1.3 \text{ meV}$ is a low temperature scattering rate, associated with a small angle scattering on the remote impurities. We attribute the quadratic temperature dependence of the single electron scattering rate to the electron-electron ($e-e$) interactions. Indeed, in a clean limit [$\tau^{-1}(0) \ll T \ll \epsilon_F$], the $e-e$ scattering rate is given by¹¹ $\tau_{e-e}^{-1} = \alpha T^2 / \epsilon_F$ (up to small logarithmic correction), where dimensionless coefficient α is of order of unity. Due to conservation of the total momentum of an electronic system, the $e-e$ interactions practically do not change the two particle (transport) scattering rate of each well (see, however, Ref. 6 for the discussion of the dirty case). As a result, the interactions do not influence the resistance at the resonance [if $|\Delta|^2 \gg (\tau(T)\tau^{\text{tr}})^{-1}$] and very far from it. However, the *width* of the resonance, as we have demonstrated above, is sensitive to the single particle scattering rate, $\tau^{-1}(T)$. The latest is not usually measurable in any transport experiment, but it includes among the other mechanisms the electron scattering due to $e-e$ interactions. The physical reason, why the transport property (resistance) of our structure appears to be sensitive to the $e-e$ interactions, is very similar to those of small angle scattering [see our discussion after Eq. (6)]. Namely, the interactions govern degree of delocalization

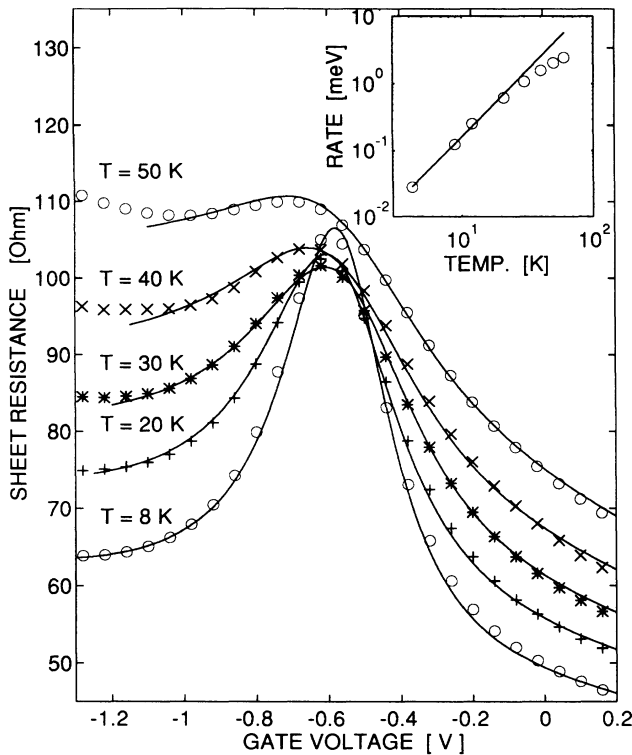


FIG. 3. The set of RR curves at different temperatures. The inset shows the variation of $\tau^{-1}(T) - \tau^{-1}(0)$ vs temperature. The circles denote the values deduced from analysis of experimental data, the solid line represents $3.0 T^2 / \epsilon_F$ (meV).

of electrons between the clean and the dirty QW's, hence altering the ability of the clean well to shunt the dirty one. Thus, we conclude that the RR is a powerful method of measuring of e - e scattering rate.

The Hall effect measurements are necessary to establish parameters of the structure. They are, however, interesting due to a presence of a "negative" resonance in a Hall coefficient. The experimental data for the Hall coefficient, R_H , at $T = 4.2$ K and magnetic field less than 0.05 T (the region, where a Hall voltage is linear with field) is presented in Fig. 4 (circles). The theoretical curve [see Eq. (7)] is also plotted on the same graph by a solid line. The nature of the "negative" resonance may be easily understood using a classical two-band model.¹²

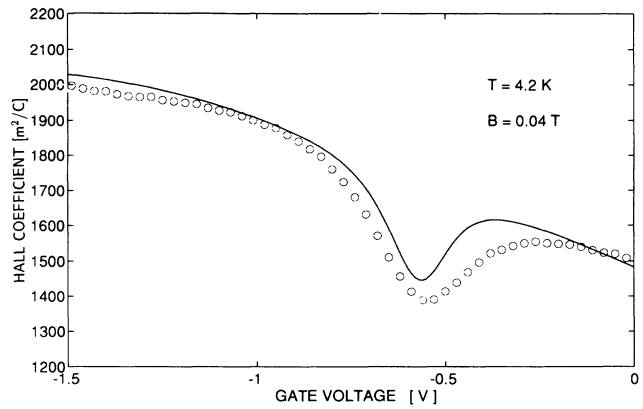


FIG. 4. Hall coefficient vs gate voltage: circles—experimental data, solid line—theoretical calculation.

According to this model, two bands having concentration of carriers n_i and transport times τ_i^{tr} , exhibit the following Hall coefficient

$$R_H = (1/e) \{ [n_1(\tau_1^{tr})^2 + n_2(\tau_2^{tr})^2] / (n_1\tau_1^{tr} + n_2\tau_2^{tr})^2 \}. \quad (9)$$

Far from the resonance the role of two bands are played by two QW's, thus, in this case, n_i and τ_i^{tr} are characteristics of uncoupled wells [cf. Eq. (7)]. In the exact resonance the two bands are symmetric and antisymmetric subbands, which obviously have the same transport times, τ^{tr} , and practically the same concentrations, n ($\Delta \ll \epsilon_F$); thus, in the resonance, $R_H = (2en)^{-1}$ [in agreement with Eq. (7)]. If the concentrations in the two wells differ from each other slightly ($n_1 \approx n_2 \approx n$), the resonance value of the Hall coefficient is strictly less than the off-resonance one. Another prediction of the simple two-band model is the dependence of a Hall coefficient on a magnetic field.¹² This was also observed experimentally in a full agreement with a model, confirming that a classical two-band model is applicable to our structure.

We have benefited from the useful discussions with A. Aronov, O. Entin, V. Fleurov, Y. Gefen, and Y. Levinson. The experimental research was supported by Israel Academy of Sciences and Humanities. A.K. was supported by the German-Israel Foundation (GIF) and the U.S.-Israel Binational Science Foundation (BSF).

¹ A. Palevski *et al.*, Phys. Rev. Lett. **65**, 1929 (1990).

² A. Palevski *et al.*, Superlatt. Microstruct. **11**, 269 (1992).

³ Y. Ohno *et al.*, Appl. Phys. Lett. **62**, 1952 (1993).

⁴ A. A. Abrikosov *et al.*, *Methods of Quantum Field Theory in Statistical Physics* (Prentice-Hall, Englewood Cliffs, NJ, 1963).

⁵ H. Fukuyama, J. Phys. Soc. Jpn. **49**, 644 (1980).

⁶ B. L. Altshuler and A. G. Aronov, in *Electron-Electron Interaction in Disordered Systems*, edited by A. J. Efros and M. Pollak (Elsevier, Amsterdam, 1985), pp. 1-153.

⁷ The mobility of a dirty well decreases linearly with electron concentration, cf. W. Walukiewicz, H. E. Ruda, J.

Lagowski, and H. C. Gatos, Phys. Rev. B **30**, 4571 (1984). This dependence was verified in a weak parallel magnetic field, where the RR is practically suppressed [Y. Berk *et al.* (unpublished)].

⁸ G. S. Boeinger *et al.*, Phys. Rev. B **43**, 12 673 (1991).

⁹ P. T. Coleridge, Phys. Rev. B **44**, 3793 (1991).

¹⁰ L. N. Pfeiffer *et al.*, Appl. Phys. Lett. **55**, 1888 (1989).

¹¹ G. F. Giuliani and J. J. Quinn, Phys. Rev. B **26**, 4421 (1982).

¹² N. W. Ashcroft and N. D. Mermin, *Solid State Physics: Advances in Research and Applications* (Saunders, Philadelphia, 1976) p. 240.

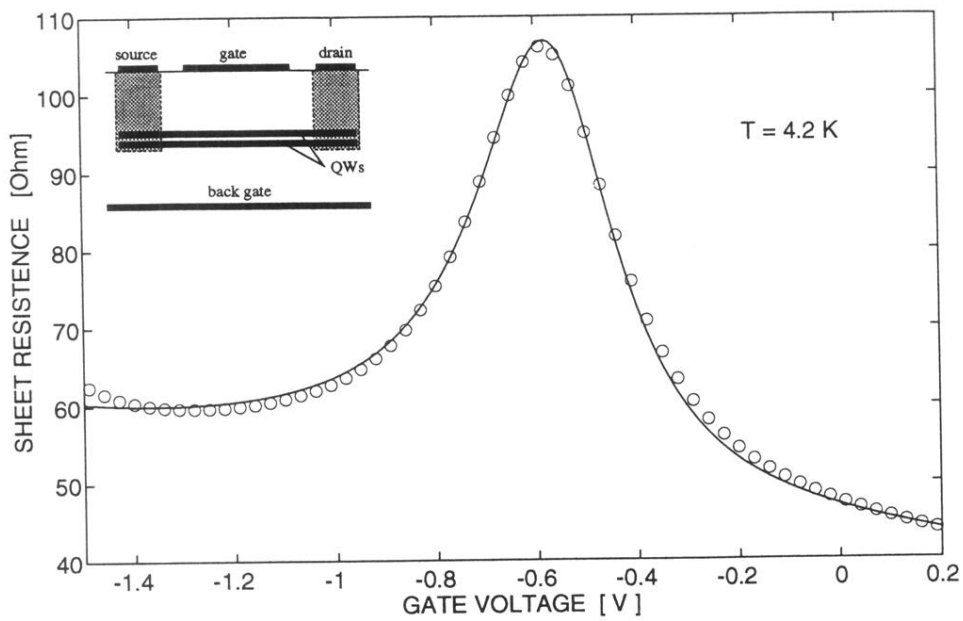


FIG. 1. Resistance resonance (RR) curves: circles—experimental data, solid line—theoretical calculation. The inset—schematic diagram of the device.